

Markov random field model and expectation of maximization for images segmentation

Lalaoui Lahouaoui, Djaalab Abdelhak

Department of Electronics Faculty of Technology, University Mohamed Boudiaf of Msila, Msila, Algeria

Article Info

Article history:

Received May 14, 2022

Revised Oct 11, 2022

Accepted Oct 20, 2022

Keywords:

Criteria evaluation

EM methods

ICM algorithm

Image segmentation

Markov random fields

ABSTRACT

Image segmentation is a significant issue in image processing. Among the various models and approaches that have been developed, some are commonly used the Markov random field (MRF) model, statistical techniques MRF. In this study a Markov random field proposed is based on an expectation-maximization (EM) modified (EMM) model. In this paper, the local optimization is based on a modified EM method for parameter estimation and the iterative conditional model (ICM) method for finding the solution given a fixed set of these parameters. To select the combination strategy, it is necessary to carry out a comparative study to find the best result. The effectiveness of our proposed methods has been proven by experimentation. We have applied this segmented algorithm to different types of images, exhibiting the algorithm's image segmentation strength with its best values criteria for EM statics and other methods.

This is an open access article under the [CC BY-SA](#) license.



Corresponding Author:

Lalaoui Lahouaoui

Department of Electronics Faculty of Technology, University Mohamed Boudiaf of Msila

2800 city ichbilia, Msila, Algeria

Email: lahouaoui.lalaoui@univ-msila.dz

1. INTRODUCTION

Now in the word, methods of medical image acquisition methods have advanced rapidly, including magnetic resonance imaging (MRI), computed tomography (CT), ultrasound (US), positron emission tomography (PET), and single photon emission tomography are some of the imaging techniques. Markov random fields in image segmentation is a book that covers the principles of markovian modeling in image segmentation and provides a quick summary of current achievements in the subject. Image labeling is a common framework in which segmentation is considered, when the task is simplified to labeling pixels. With the production more and more of image medical, image automated, processing and analysis techniques have become increasingly important [1]. In the field of probability, it is possible to introduce a segmentation class where the characteristics of regions can be modeled by MRF. The major drawback of the Markov field model is that the approximation algorithms they induce are iterative and very computationally intensive. To reduce the amount of computation and obtain non-iterative computational algorithms, we can use hidden Markov chains [2]-[4], or with Gaussian mixture models (GMM) [5], [6], or with conditional random fields conditional random field (CRF) [7], [8].

Although optical, robotics has made extensive use of image processing technology most of these methods cannot be used to process medical images. Image segmentation is the process of dividing an image into multiple segments to simplify the representation of the image or extract meaningful objects. Image segmentation is one of the most important roles in computer vision, and it has several applications in domains such as pattern recognition, remote sensing, and machine learning, medical diagnostics and computer vision, remote sensing, and medical imaging. A fuzzy treatment of masked image segmentation with MRF model

has been proposed [9]-[12]. Thus, this work is novel in three ways. i) we offer an estimation and prediction of interface levels. Approach based on MRF, ii) a method for simultaneously estimating GMM parameters using the EM Algorithm to account for MRF spatial constraints; and iii) validation of proposed methods on medical and synthetic images [13].

The MRF model MRF [14] is a probabilistic graphical model that provides a statistical framework for modeling spatial contextual constraints as prior information. The spatially contextual MRF model is time-consuming and cannot describe long-distance interactions between pixels, i.e., a macro texture model. The region-based MRF, on the other hand, can use region-based information to capture the macro texture pattern, but it suffers from irregular spatial context. To achieve accurate measurement of the interface in real-time, we use an approach based on Gaussian mixture models and MRF based on unsupervised image segmentation [15]-[17]. Image processing tasks such as image segmentation have proven to be suitable for MRFs, [18]. One for the background and one for the foreground GMM, replaced the user's seed histograms and to fix the transparency on the edges of segmented objects, a border matting algorithm was developed [19]-[21].

The region-level MRF model has been proposed with an approach for the fusion using the FCM clustering algorithm based on the MRF, multispectral and panchromatic images are exploited for local spatial information [22]-[25]. Their concept of label uncertainty, however, cannot be applied to generic MRF models. A general concept of uncertainty in the context of image segmentation can be defined as the variance or inequality [26] in the label assignments resulting from the label image's distribution posterior. To solve the MAP problem, the iterative conditional model (ICM) is used; this method is compared to traditional expectation-maximization (EM) and MRF image segmentation techniques using synthetic and real images [27], [28]. The approximation algorithms they induce are iterative and very computationally intensive. The joint field of expectation of maximization field and MRF are designed to optimize image segmentation results, which can improve image segmentation accuracy.

The rest of the research paper is organized as shown in: Section 2 provides a brief overview of the MRF model, while section 3 presents the new regional feature of the MRF model as well as details of the EMRF model. Section 5 describes the algorithm. Section 3 contains the results of the experiments, and section 4 contains the conclusion.

2. MATERIALS AND METHOD

2.1. Framework MRF

Markov random field theory provides a handy and coherent framework method for modeling image pixels and linked features are examples of context-dependent entities. Improved maximum a posteriori expectation-maximization (MAP-EM) image segmentation algorithm that calculates the proportion of tissue mixture within each picture voxel as well as tissue distribution statistical model parameters [29]. It may be viewed as a labeling issue for segmentation, with the segmented result generated by maximizing the posterior estimation of the labeling problem. By synthesizing the maximum, a posteriori (MAP) solution and incorporating prior information, the Bayesian framework aids in the generation of statistical inferences. The purpose of the MAP solution is to maximize the posterior probability, which is written as:

MRF framework: Given a group of pixels $S = \{s_1 \dots s_m\}$ and group of labels $\Delta = \{l_1 \dots l_L\}$ and neighborhood system N , find the mapping of S to Δ .

Let K be the configuration for labels,

$$M = \{l_1 \dots l_2\}, m_i \in \Delta \text{ is the label for } s_1.$$

M is MRF concerning N iff:

- Positivity: $P(M = m) \geq 0 \forall m \in M$.
- Markovianity:

$$P(M_s = m_s / M_r = m_r, \forall r \neq s) = P(M_s = m_s / M_r = m_r, \forall r \in N_s) \tag{1}$$

Let G be the observed image.

$$G = \varphi(H(M) + N)$$

Where H =camera transfer function and φ =Recorder distortion, h is assumed to be LSI and φ is invertible nonlinear function and N is additive noise. In the framework of restoration: Given G what is F ?; $P(M = \frac{m}{G} = g)$, Maximum likelihood of: $M = m$ given; $G = g$. From Bays rule:

$$P\left(M = \frac{m}{G} = g\right) \propto P\left(G = \frac{g}{m} = M\right) P(M = m) \quad (2)$$

where $P\left(G = \frac{g}{m} = M\right)$ = data model, $P(M = m)$ = prior and $P\left(M = \frac{m}{G} = g\right)$ = Aposteriori distribution. Need to maximize posterior (MAP) distribution:

$$P(k) = (1/Z) \exp(-U(m)/T) \quad (3)$$

$U(M) = \sum_{c \in N} V_c(m)$ **IS energy function**, where V_c : **clique** Potentiel:

$$Z = \sum_f (1/Z) \exp(-U(M)/T) \quad (4)$$

Z: partition Function, and T= Temperature.

Hammersley Clifford theorem M is MRF on S concerning N if and only if M is Gibbs random field on S forl. Relates conditional distribution (Local characteristic joint distribution (Gibbs measure)).

$$\arg \max_{m \in M} P(f | d) \quad (5)$$

If computed over all cliques, it would take a long time. In practice, it is common to execute the computation over single and pair site cliques.

2.2. The MRF model

The Markov field technique attempts to account for term dependency. It's also known as an undirected graphical model. This method is widely used in machine learning. This method is used in IR to describe term dependencies, such as dependence sequence and complete dependency.

2.3. The proposed algorithms

In the EM algorithm simulated field. Input: an observation y, some iterations T. Output: an estimate of the likelihood maximum estimator $\hat{\theta}$ MLE. Initialization: start to form an initial guess $\theta^{(0)} = (\theta^{(0)}, \phi^{(0)})$, do Neighbourhood restoration: draw $\hat{\theta}^{(t)}$ from $\pi(\cdot | y, \theta^{(t-1)}, \phi)$.

E-step: Estimate the expected value for each latent variable. We compute:

$$\hat{\theta}_1(\phi) = \sum_{i \in \mathcal{L}} \sum_{x_i} P(x_i; \hat{X}_{N(i)}^{(t)}, y_i, \psi^{(t-1)}, \phi) \log_{\phi} p(y_i | x_i) \quad (6)$$

$$\hat{\theta}_1(\phi) = \sum_{i \in \mathcal{L}} \sum_{x_i} P(x_i; \hat{X}_{N(i)}^{(t)}, y_i, \psi^{(t-1)}, \mathcal{L}) \log P(x_i; \hat{X}_{N(i)}^{(t)}, y_i, \theta, \mathcal{L}) \quad (7)$$

M-Step. Optimize the parameters of the distribution using maximum likelihood. set of parameters, k denotes the Gaussian component of the mixture model, K denotes the total number of Gaussian distributions in the mixture model. w_m is the weight of each Gaussian distribution that meets M, $m=1$, and $w_m=1$.

θ : old, θ' : New,

$$\begin{aligned} \phi(\theta, \theta') &= \sum_y p_{\theta'}\left(\frac{y}{x}\right) \cdot \log p_{\theta}(y, x) = \sum_y \frac{p_{\theta'}(y, x)}{p_{\theta'}(x)} \log p_{\theta}(y, x) \\ &= \sum_y p_{\theta'}\left(\frac{y}{x}\right) \log(p_{\theta}\left(\frac{y}{x}\right) p_{\theta}(x)) = \sum_y p_{\theta'}\left(\frac{y}{x}\right) \left[\log p_{\theta}\left(\frac{y}{x}\right) + \log p_{\theta}(x) \right] \\ &= \sum_y p_{\theta'}\left(\frac{y}{x}\right) \log p_{\theta}\left(\frac{y}{x}\right) + \sum_y p_{\theta'}\left(\frac{y}{x}\right) \log p_{\theta}(x) \end{aligned} \quad (8)$$

$$\log p_{\theta}\left(\frac{y}{x}\right) \leq \frac{y}{x} - 1; \log p_{\theta}(x) \leq x - 1$$

$$\phi(\theta, \theta') \leq \sum_y p_{\theta'}\left(\frac{y}{x}\right) \left(\frac{y}{x} - 1\right) + \sum_y p_{\theta'}\left(\frac{y}{x}\right) (x - 1) \quad (9)$$

$$\phi(\theta, \theta') \leq \sum_y p_{\theta'}\left(\frac{y}{x}\right) \cdot \frac{y}{x} - \sum_y p_{\theta'}\left(\frac{y}{x}\right) + \sum_y p_{\theta'}\left(\frac{y}{x}\right) \cdot x - \sum_y p_{\theta'}\left(\frac{y}{x}\right) \quad (10)$$

$$\phi(\theta, \theta') \leq \sum_y p_{\theta'}\left(\frac{y}{x}\right) \cdot \frac{y}{x} + \sum_y p_{\theta'}\left(\frac{y}{x}\right) \cdot x - 2 \sum_y p_{\theta'}\left(\frac{y}{x}\right) \quad (11)$$

$$\phi(\theta, \theta') \leq \sum_y p_{\theta'}\left(\frac{y}{x}\right) \cdot \frac{y}{x} + (x - 2) \sum_y p_{\theta'}\left(\frac{y}{x}\right) \quad (12)$$

end,

$$\phi^{(T)} = (\theta^{(T)}, \phi^{(T)}) \tag{13}$$

that is,

$$P(X = x) = (1/Z)\exp(-U(x)) \tag{14}$$

$$\text{Where } Z = \sum_x U(x) \tag{15}$$

is the normalization factor and,

$$U(x) = \sum_{s \in S} U(x_s, x_{Ns}) \tag{16}$$

is the energy function. Here:

$$U(x_s, x_{Ns}) = \sum_{t \in N} V(x_s, x_t) \tag{17}$$

where N_s is a group of sites adjacent to site s and $V(x_s, x_t)$ is the potential function between site s and site t , $t \in N_s$. Typically, the multilevel logistic (MLL) model [30] is used to define the potential function: $V(x_s, x_t)$ which is:

$$V(x_s, x_t) = \beta \text{ if } x_s = x_t = -\beta \text{ if } x_s \neq x_t, \tag{18}$$

where $\beta > 0$ denotes the potential parameter and $t \in N_s$. According to the MLL model, $P(X)$ has a large value if the local neighbor labels are the same, otherwise it has a small value. It is used to calculate the probability that the observed image Y corresponds to the given realization $X = x$. That is:

$$P(Y|X = x) = \prod_{s \in S} P(y_s|x) = \prod_{s \in S} P(y_s|x_s) \tag{19}$$

segmentation consists in estimating μ knowing the observed image a . You can use a Bayesian approach which consists in finding the most probable class in the sense of the probability at posterior obtained by maximizing $P(y_s = \mu | x_s = \Gamma)$. It is therefore a matter of constructing $P(x_s = \Gamma | y_s = \mu)$, then fix a prior law on μ , denoted $P(\mu = \Gamma)$, from which we calculate $P(y_s = \mu | x_s = \Gamma)$ by of Bayes.

$$P(y_s|x_s) = (2\pi)^{-D/2} \exp - 1/2 (y_s - \mu)^T \Gamma^{-1} (y_s - \mu) \tag{20}$$

3. RESULTS AND DISCUSSION

The obtained results are presented in the Figure 1 to Figure 3, where we have presented the segmentation evaluation criteria in Table 1. It is concluded that the ICM algorithm based on the EM method performs better compared to the ICM based on the method for K-means image real. In this section, the proposed algorithm is applied to synthetic and real images. We present the results of the application of improved MRF based on modified EM algorithms. Our proposed technique has been tested on several different images. Figure 1 shows the input images and image segmentation obtained by our method. It is clear that the results using the proposed technique had good quality and were better than those using the classical method. The performance of these algorithms is compared to the standard versions of the MRF and EM algorithms. We present the results obtained for image segmentation by Markov fields based on EM and changed EM algorithms. For output image evaluation, not only visual comparison but also quantitative measurements such as entropy, mean square error (MSE), and peak signal to noise ratio (PSNR) are used to evaluate the output image. To make an objective comparison of the different proposed methods, we propose to use the following as evaluation criteria: mean squared error (MSE), signal to noise ratio PSNR, normalized cross-correlation (NCC), structural content (SC) and normalized absolute error (NAE). We present in tables the values of the validation criteria for all the proposed methods. This will be followed by an interpretation of the results to be able to make a comparison between the used segmentation methods. First, we define the evaluation criteria that we mentioned above. The methods of assessing image quality can be classified into three broad categories: The most widely used quantitative measures are the mean squared error (MSE), the peak signal-to-noise ratio (PSNR), and the signal-to-noise ratio (hat the ICM algorithm based on the EM method performs better compared to the ICM algorithm based on the method for K-means image real. In this section, the proposed algorithm is applied to synthetic and real images. We present the results of the application of improved MRF based on modified EM algorithms. Our proposed technique has been tested on several different images. Figure 1 shows the input images and image segmentation obtained by our method. It

is clear that the results using the proposed technique had good quality and were better than those using the classical method. The performance of these algorithms is compared to the standard versions of the MRF and EM algorithms. We present the results obtained for image segmentation by Markov fields based on EM and changed EM algorithms. For output image evaluation, not only visual comparison but also quantitative measurements such as entropy, mean square error (MSE), and PSNR are used to evaluate the output image. To make an objective comparison of the different proposed methods, we propose to use the following as evaluation criteria: MSE, PSNR, NCC, SC, and NAE. It is based on measuring the MSE computed between the original pixels and the degraded ones: The MSE is equal to 0 if a model has no errors. Its value rises in proportion to the model error. Additionally known as the mean squared deviation (MSD), the mean squared error.

Where $(M \times N)$ is the size of the image, I_p and \hat{I}_p are respectively the amplitudes of the pixels on the original and degraded images. The eye likely takes more account of errors in large amplitudes, which promotes the quadratic measure. The PSNR is to quantify the performance of the algorithms by measuring the quality of reinsertion of the segmented image compared to the original image.

PSNR levels for high-quality images typically range between 30 and 40 dB. A greater SC rating indicates that the image is of low quality. The NCC calculation compares the processed picture to the reference image. Finally, the greater the value of the maximum difference, the better the image quality. This quality metric may be stated as follows: This measure of quality can be stated as follows: A higher price NAB demonstrates that the image quality is low.

3.1. Synthetic images segmentation

In this part, we started to apply the two segmentation methods to the synthetic images, and after that, we evaluated these methods by evaluation criteria that we saw previously. From the values in Table 1, (PSNR=7.9280) and (SC=1.5034) we see that the quality of the segmented image is poor by the ICM method based on the EM algorithm versus ICM. An infinite PSNR value corresponds to an undegraded image. In addition, this value decreases according to the degradation of the PSNR and therefore links with MSE the maximum energy of the image. Regardless of the value of MSE, the value of PNSR is large. In Figure 1(a), we presented the synthetic image original, these results obtained after segmentation with MRF-based EM (in Figure 1(b), and Segmentation with MRF-based EM algorithm in Figure 1(c). From the values obtuned in Table 1 (PSNR=7.9280) and (SC=0.2115) where we can see that the quality of the segmented image is poor from the ICM method based on the EM algorithm. Table 1 presented the two algorithms used for synthetic image segmentation with EM and EM modified.

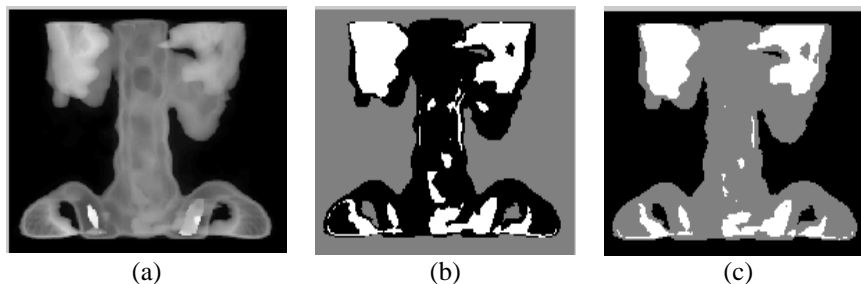


Figure 1. Result obtuned of simulation methods for synthetic images, (a) image original, (b) segmentation with MRF-based EM, and (c) segmentation par MRF-based modified EM algorithm

Whatever the value of MSE, the value of PNSR is great. In Table 1, we present also the values of different criteria used here such as MSE, NCC, SC, PSNR, and NAE for the EM and EM modified used in Markov field random. Figure 2 presented the bare for criteria MSE, PSNR, NCC, SC and NAE obtained from the synthetic image segmentation algorithm.

Table 1. Values of the evaluation criteria for image segmentation

Criteria	EM modified	EM
MSE	1.6607	1.1209
PSNR	7.9280	7.6352
NCC	2.0332	1.9389
SC	0.2115	0.2501
NAE	1.0332	0.9389

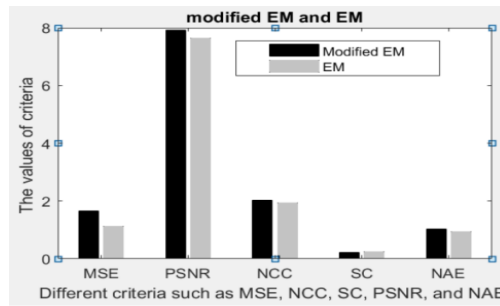


Figure 2. We present here the accuracy criteria such as (MSE, PSNR, NCC, SC, and NAE) obtained with MRF based on EM, and MRF based on the modified EM for the image synthetic

3.2. Real image segmentation

In this part, we started to apply the two segmentation methods to real images and synthetic images and then we evaluated these methods by evaluation criteria that we have seen previously. The obtained results are depicted in Table 2 and it shows that the ICM algorithm based on the modified EM method is better compared to ICM based method for EM on the actual images. To benefit from the advantages of the two methods presented in the previous paper, we decided to use them to segment the images, and we made a table for each result. Table 2 presents the values of some evaluation criteria on the segmentation results with the two optimal values (taking into account the direction of variation of the criteria).

Table 2 presented the value of different criteria used here such as MSE, NCC, SC, PSNR, and NAE for the EM and EM modified used in Markov field random. Figure 3 presented the two algorithms used for synthetic image segmentation with EM and EM modified. In Figure 3(a), we presented the reel image original, these results obtained after segmentation with MRF-based EM in Figure 3(b), and Segmentation with MRF-based modified EM algorithm in Figure 3(c). From the values in the Table 2 (PSNR = 6.925) and (SC = 0.2349) in can see that the quality of the segmented image is poor by the ICM method based on the EM algorithm versus ICM.

Figure 4 presents the bare for MSE, PSNR, NCC, SC, and NAE criteria obtained from the synthetic image segmentation algorithm. To benefit from the advantages of the two methods presented in the previous section, we decided to use them to segment the images. And we made a table for each result; this table shows the values of some evaluation criteria on segmentation results both optimal values (considering the direction of change of criteria). We can see in Figure 4 that the interest of the segmentation method KMeans it will keep precise borders. The outline image as it appears is a typical image for this kind of segmentation with similar EMs. The values of KMeans are large relative to the value of EM. Therefore, the quality is good and the best EM algorithm. It is possible to deduce that the ICM algorithm based on EM method is better compared to ICM based on the method for K-means images the values of the criteria give the information that the EM algorithm is better than the K-means algorithm.

Table 2. The Values of criteria for image segmentation

Criteria	EM modified	EM
MSE	1.3199	1.5917
PSNR	6.925	6.1122
NCC	1.9689	1.8724
SC	0.2349	0.2305
NAE	0.96890	0.8724

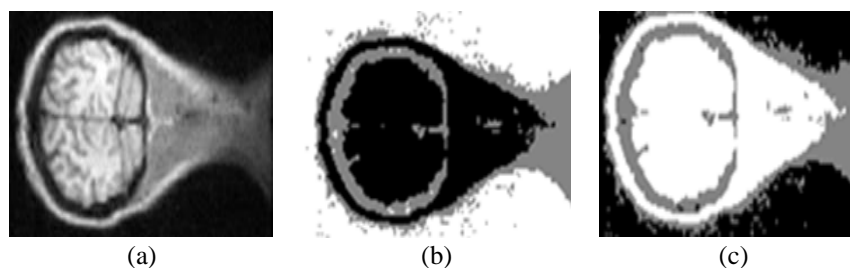


Figure 3. Result obtained with simulation for real images, (a) image original, (b) segmentation with MRF based on EM, and (c) MRF based on modified EM

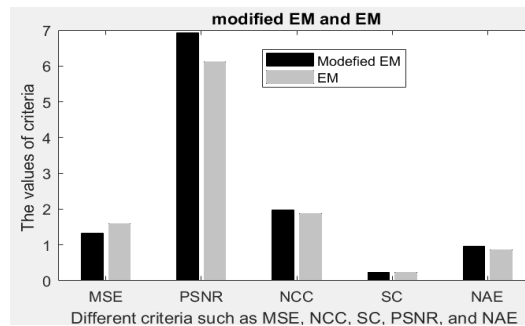


Figure 4. We present here the accuracy criteria such as (MSE, PSNR, NCC, SC, and NAE) obtained with MRF based on EM, and MRF based on the modified EM for the image real

4. CONCLUSION

In current work, we have considered various segmentation tasks in an image labeling framework, where the challenge is simplified to labeling pixels. The labels were modeled using MRF in a probabilistic approach, and inference is performed using Bayesian estimation, specifically a MAP. MRF modeling has the advantage of allowing a priori information to be "coded" locally by click potentials. We exploit the results obtained by different methods such as Markov fields based on the EM and modified EM algorithms for image segmentation. Experimental evaluations on multiple reference sources and target datasets indicate that this is efficient for image segmentation. We proposed a method for improving the image's grayscale and image detail by using quantitative measures to analyze the output image, such as entropy, MSE, and PSNR. Image processing is a research subject located between computer science and signal processing. In current work, we have presented various algorithms for based-region segmentation. Whether sequential or mutual, cooperative segmentation uses a single type of information per region to allow better consideration of the characteristics of the objects in the image. The region-wise approach consists in bringing together the associated pixels in a homogeneous region; it is based on the notion of similarity. It's quick and easy, but using only local MRF information based on EM to assess these results, we used the following criteria: MSE, PNSR, NCC, SC, MD, and NAE, and two algorithms: EM and EM amended. In this work, we presented the results of the region segmentation algorithm based on Markov fields. The obtained results show that the MRF method based on modified EM is better than that based on classical EM. Nevertheless, many image segmentation tasks can be formulated under these constraints.





REFERENCES

- [1] Z. Jiang, M. Xie, and A. M. Sainju, "Geographical Hidden Markov Tree," *IEEE Transactions on Knowledge and Data Engineering*, vol. 33, no. 2, pp. 506–520, 2021, doi: 10.1109/TKDE.2019.2930518.
- [2] R. C. Dubes, A. K. Jain, S. G. Nadabar, and C. C. Chen, "MRF model-based algorithms for image segmentation," in *Proceedings - International Conference on Pattern Recognition*, 1990, vol. 1, pp. 808–814, doi: 10.1109/icpr.1990.118221.
- [3] Q. Zhao, X. Li, Y. Li, and X. Zhao, "A fuzzy clustering image segmentation algorithm based on Hidden Markov Random Field models and Voronoi Tessellation," *Pattern Recognition Letters*, vol. 85, pp. 49–55, Jan. 2017, doi: 10.1016/j.patrec.2016.11.019.
- [4] Y. Hou, L. Guo, and X. Lun, "A Novel MRF-Based Image Segmentation Algorithm," in *2006 9th International Conference on Control, Automation, Robotics and Vision*, 2006, pp. 1–5, doi: 10.1109/ICARCV.2006.345105.
- [5] H. Gribben, P. Miller, G. G. Hanna, K. J. Carson, and A. R. Hounsell, "Map-Mrf Segmentation of lung tumours in pet/ct images," in *Proceedings - 2009 IEEE International Symposium on Biomedical Imaging: From Nano to Macro, ISBI 2009*, Jun. 2009, pp. 290–293, doi: 10.1109/ISBI.2009.5193041.
- [6] S. Ryali, T. Chen, K. Supekar, and V. Menon, "A parcellation scheme based on von Mises-Fisher distributions and Markov random fields for segmenting brain regions using resting-state fMRI," *NeuroImage*, vol. 65, pp. 83–96, Jan. 2013, doi: 10.1016/j.neuroimage.2012.09.067.
- [7] A. B. Ashraf, S. C. Gavenonis, D. Daye, C. Mies, M. A. Rosen, and D. Kontos, "A multichannel Markov random field framework for tumor segmentation with an application to classification of gene expression-based breast cancer recurrence risk," *IEEE Transactions on Medical Imaging*, vol. 32, no. 4, pp. 637–648, Apr. 2013, doi: 10.1109/TMI.2012.2219589.
- [8] A. Ahmadvand and M. R. Daliri, "Improving the runtime of MRF based method for MRI brain segmentation," *Applied Mathematics and Computation*, vol. 256, pp. 808–818, Apr. 2015, doi: 10.1016/j.amc.2015.01.053.
- [9] S. Yousefi, R. Azmi, and M. Zahedi, "Brain tissue segmentation in MR images based on a hybrid of MRF and social algorithms," *Medical Image Analysis*, vol. 16, no. 4, pp. 840–848, May 2012, doi: 10.1016/j.media.2012.01.001.
- [10] B. Sridhar, K. V. V. S. Reddy, and A. M. Prasad, "Automated Medical image segmentation for detection of abnormal masses using Watershed transform and Markov random fields," *International Journal on Signal and Image Processing*, vol. 4, no. 3, p. 56, 2013, [Online]. Available: <http://searchdl.org/public/journals/2013/IJSIP/4/3/1293.pdf>.
- [11] J. Simmons, C. Przybyla, S. Bricker, D. W. Kim, and M. Comer, "Physics of MRF regularization for segmentation of materials microstructure images," in *2014 IEEE International Conference on Image Processing, ICIP 2014*, Oct. 2014, pp. 4882–4886, doi: 10.1109/ICIP.2014.7025989.





- [12] O. Yousif and Y. Ban, "Improving SAR-based urban change detection by combining MAP-MRF classifier and nonlocal means similarity weights," *IEEE Journal of Selected Topics in Applied Earth Observations and Remote Sensing*, vol. 7, no. 10, pp. 4288–4300, Oct. 2014, doi: 10.1109/JSTARS.2014.2347171.
- [13] M. Y. Siyal and L. Yu, "An intelligent modified fuzzy c-means based algorithm for bias estimation and segmentation of brain MRI," *Pattern Recognition Letters*, vol. 26, no. 13, pp. 2052–2062, Oct. 2005, doi: 10.1016/j.patrec.2005.03.019.
- [14] O. Ocegueda, T. Fang, S. K. Shah, and I. A. Kakadiaris, "3D face discriminant analysis using gauss-markov posterior marginals," *IEEE Transactions on Pattern Analysis and Machine Intelligence*, vol. 35, no. 3, pp. 728–739, Mar. 2013, doi: 10.1109/TPAMI.2012.126.
- [15] C. Wang, J. Ni, X. Zhang, and Q. Huang, "Efficient compression of encrypted binary images using the Markov random field," *IEEE Transactions on Information Forensics and Security*, vol. 13, no. 5, pp. 1271–1285, May 2018, doi: 10.1109/TIFS.2017.2784379.
- [16] G. Xia, C. He, and H. Sun, "An unsupervised segmentation method using Markov random field on region adjacency graph for SAR images," in *2006 CIE International Conference on Radar*, Oct. 2006, pp. 1–4, doi: 10.1109/ICR.2006.343148.
- [17] Y. L. Chen, T. W. Huang, K. H. Chang, Y. C. Tsai, H. T. Chen, and B. Y. Chen, "Quantitative analysis of automatic image cropping algorithms: A dataset and comparative study," in *Proceedings - 2017 IEEE Winter Conference on Applications of Computer Vision, WACV 2017*, Mar. 2017, pp. 226–234, doi: 10.1109/WACV.2017.32.
- [18] C. M. Bishop, *Pattern Recognition and Machine Learning*, 1st ed. Springer New York, 2006.
- [19] H. Derin and H. Elliott, "Modeling and segmentation of noisy and textured images using gibbs random fields," *IEEE Transactions on Pattern Analysis and Machine Intelligence*, vol. PAMI-9, no. 1, pp. 39–55, 1987, doi: 10.1109/TPAMI.1987.4767871.
- [20] S. Tongbram, B. A. Shimray, and L. S. Singh, "Segmentation of image based on k-means and modified subtractive clustering," *Indonesian Journal of Electrical Engineering and Computer Science (IJECS)*, vol. 22, no. 3, p. 1396, Jun. 2021, doi: 10.11591/ijeecs.v22.i3.pp1396-1403.
- [21] R. Usha and K. Perumal, "A modified fractal texture image analysis based on grayscale morphology for multi-model views in MR Brain," *Indonesian Journal of Electrical Engineering and Computer Science (IJECS)*, vol. 21, no. 1, pp. 154–163, Jan. 2021, doi: 10.11591/ijeecs.v21.i1.pp154-163.
- [22] D. M. Tsai and C. T. Lin, "Fast normalized cross correlation for defect detection," *Pattern Recognition Letters*, vol. 24, no. 15, pp. 2625–2631, Nov. 2003, doi: 10.1016/S0167-8655(03)00106-5.
- [23] G. Swain, "Steganography in digital images using maximum difference of neighboring pixel values," *International Journal of Security and its Applications*, vol. 7, no. 6, pp. 285–294, Nov. 2013, doi: 10.14257/ijasia.2013.7.6.29.
- [24] T. Blaskovics, Z. Kato, and I. Jermyn, "A Markov random field model for extracting near-circular shapes," in *Proceedings - International Conference on Image Processing, ICIP*, Nov. 2009, pp. 1073–1076, doi: 10.1109/ICIP.2009.5413472.
- [25] W. Tao, F. Chang, L. Liu, H. Jin, and T. Wang, "Interactively multiphase image segmentation based on variational formulation and graph cuts," *Pattern Recognition*, vol. 43, no. 10, pp. 3208–3218, Oct. 2010, doi: 10.1016/j.patcog.2010.04.014.
- [26] S. Han, W. Tao, and X. Wu, "Texture segmentation using independent-scale component-wise Riemannian-covariance Gaussian mixture model in KL measure based multi-scale nonlinear structure tensor space," *Pattern Recognition*, vol. 44, no. 3, pp. 503–518, Mar. 2011, doi: 10.1016/j.patcog.2010.09.006.
- [27] Y. Zhang, M. Brady, and S. Smith, "Segmentation of brain MR images through a hidden Markov random field model and the expectation-maximization algorithm," *IEEE Transactions on Medical Imaging*, vol. 20, no. 1, pp. 45–57, 2001, doi: 10.1109/42.906424.
- [28] X. Taisong, Z. Lei, and Y. hang, "Double Gaussian mixture model for image segmentation with spatial relationships," *Journal of Visual Communication and Image Representation*, Volume 34, pp. 135-145, 2016, doi.org/10.1016/j.jvcir.2015.10.018.
- [29] Z. L. H. Kodamana and A. A. B. Huang, "A GMM-MRF based image segmentation approach for interface level estimation," *IFAC-PapersOnLine*, vol. 52, no. 1, pp. 28–33, 2019, doi: 10.1016/j.ifacol.2019.06.061.
- [30] S. Wang, L. Li, H. Cohen, S. Mankes, J. J. Chen, and Z. Liang, "An EM approach to MAP solution of segmenting tissue mixture percentages with application to CT-based virtual colonoscopy," *Medical Physics*, vol. 35, no. 12, pp. 5787–5798, Nov. 2008, doi: 10.1118/1.3013591.

BIOGRAPHIES OF AUTHORS



Lalaoui Lahouaoui     is a full-time lecturer at the Department of Electronics, Mohamed boudiaf University, Algeria. He received a PhD in Electronics University the Setif, from Algeria. His research interests include image/signal processing, biometrics, medical image and analysis, and pattern recognition. He can be contacted at email: lahouaoui.lalaoui@univ-msila.dz.



Djaalab Abdelhak     is a full-time lecturer at the Department of Electronics, Mohamed Boudiaf University from Algeria. His research interests include image/signal processing, biometrics, medical image and analysis, and pattern recognition. He can be contacted at email: abdelhak.djaalab@univ-msila.dz and zino4525@yahoo.fr.